Role of sarcolemmal ATP-sensitive K^+ channels in the regulation of sinoatrial node automaticity: an evaluation using Kir6.2-deficient mice

Koichi Fukuzaki[1], Toshiaki Sato[1], Takashi Miki[2], Susumu Seino[3] and Haruaki Nakaya[1]

[1]*Department of Pharmacology and* [2]*Department of Autonomic Physiology, Chiba University Graduate School of Medicine, Chiba, Japan*
[3]*Division of Cellular and Molecular Medicine, Kobe University Graduate School of Medicine, Kobe, Japan*

The role of cardiac sarcolemmal ATP-sensitive K^+ (K_{ATP}) channels in the regulation of sinoatrial node (SAN) automaticity is not well defined. Using mice with homozygous knockout (KO) of the Kir6.2 (a pore-forming subunit of cardiac K_{ATP} channel) gene, we investigated the pathophysiological role of K_{ATP} channels in SAN cells during hypoxia. Langendorff-perfused mouse hearts were exposed to hypoxic and glucose-free conditions (hypoxia). After 5 min of hypoxia, sinus cycle length (CL) was prolonged from 207 ± 10 to 613 ± 84 ms ($P < 0.001$) in wild-type (WT) hearts. In Kir6.2 KO hearts, CL was slightly prolonged from 198 ± 17 to 265 ± 32 ms. The CL of spontaneous action potentials of WT SAN cells, recorded in the current-clamp mode, was markedly prolonged from 410 ± 56 to 605 ± 108 ms ($n = 6, P < 0.05$) with a decrease of the slope of the diastolic depolarization (SDD) after the application of the K^+ channel opener pinacidil (100 μM). Pinacidil induced a glibenclamide (1 μM)-sensitive outward current, which was recorded in the voltage-clamp mode, only in WT SAN cells. During metabolic inhibition by 2,4-dinitrophenol, CL was prolonged from 292 ± 38 to 585 ± 91 ms ($P < 0.05$) with a decrease of SDD in WT SAN cells but not in Kir6.2 KO SAN cells. Diastolic Ca^{2+} concentration, measured by fluo-3 fluorescence, was decreased in WT SAN cells but increased in Kir6.2 KO SAN cells after short-term metabolic inhibition. In conclusion, the present study using Kir6.2 KO mice indicates that, during hypoxia, activation of sarcolemmal K_{ATP} channels in SAN cells inhibits SAN automaticity, which is important for the protection of SAN cells.

(Received 27 November 2007; accepted after revision 10 April 2008; first published online 17 April 2008)
Corresponding author H. Nakaya: Department of Pharmacology, Chiba University Graduate School of Medicine, 1-8-1 Inohana, Chuo-ku, Chiba 260-8670, Japan. Email: nakaya@faculty.chiba-u.jp

ATP-sensitive K^+ (K_{ATP}) channels, originally discovered in cardiomyocytes (Noma, 1983), are present in many tissues and play an important role in various cellular functions (Seino & Miki, 2003). Recent studies have indicated that the cardiac K_{ATP} channel is a hetero-octametric complex of four pore-forming subunits (Kir6.2) and four regulatory sulphonylurea receptor (SUR2A) subunits (Seino, 1999). Several studies from our laboratory, using mice with homozygous knockout of the Kir6.2 gene (Kir6.2 KO), have demonstrated that Kir6.2 is essential for the function of K_{ATP} channels in atrial and ventricular cells (Suzuki *et al.* 2001; Saegusa *et al.* 2005). The activation of K_{ATP} channels plays an important role in the action potential shortening but not in the extracellular K^+ accumulation during myocardial ischaemia (Suzuki *et al.* 2002; Saito *et al.* 2005).

The sinoatrial node (SAN), the location of which was discovered in the mammalian heart a century ago (Keith & Flack, 1907), has spontaneous automaticity generated by the diastolic depolarization. Electrophysiological, pharmacological and genetic investigations have demonstrated that different types of membrane currents are involved in the generation of the action potential and the pacemaker activity (Irisawa *et al.* 1993; Kodama *et al.* 1997; Marionneau *et al.* 2005; Mangoni *et al.* 2006). A previous electrophysiological study showed that K_{ATP} channels exist in the rabbit SAN cells (Han *et al.* 1996). In addition, a recent study using the RT-PCR technique has indicated that Kir6.2 and SUR2 genes are expressed in mouse SAN tissue (Marionneau *et al.* 2005). However, functional roles of K_{ATP} channels are not fully understood although SAN automaticity is known to be susceptible and vulnerable to metabolic inhibition such as hypoxia (Nishi *et al.* 1980). The present study was conducted to examine whether the activation of K_{ATP} channels regulates the SAN automaticity during hypoxia or metabolic inhibition

 DOI: 10.1113/jphysiol.2007.148932

using isolated hearts and SAN cells of Kir6.2 KO mice. The use of Kir6.2-deficient mice would have an advantage because K_{ATP} channel blockers such as glibenclamide have non-specific blocking actions on the other ion channels and transporters (Rosati *et al.* 1998; Hernandez-Benito *et al.* 2001; Lee & Lee, 2005).

Methods

Kir6.2-deficient mice

A mouse line deficient in the K_{ATP} channels was generated by targeted disruption of the gene coding for Kir6.2, as previously described (Miki *et al.* 1998). C57BL/6 mice were used as controls because KO animals had been back-crossed to a C57BL/6 strain for five generations. C57BL/6 wild-type (WT) and Kir6.2-deficient (Kir6.2 KO) mice at the age of 8–14 weeks were used in this study. All procedures complied with the *Guide for the Care and Use of Laboratory Animals* (NIH Pub. no. 85-23, 1996 version) and were approved by the Institutional Animal Care and Use Committee of Chiba University.

Langendorff-perfused hearts

Mice were anaesthetized with urethane (1.5 g kg^{-1} I.P.) and anticoagulated with heparin (100 U kg^{-1} I.V.). Hearts were quickly excised and connected to the Langendorff apparatus by inserting a perfusion cannula into the aorta, as previously described (Suzuki *et al.* 2001). Retrograde perfusion was maintained at a constant pressure of 80 cmH_2O with a modified Tyrode solution containing (mM): 125 NaCl, 4 KCl, 1.8 NaH_2PO_4, 0.5 $MgCl_2$, 1.8 $CaCl_2$, 5.5 glucose and 25 $NaHCO_3$. The perfusate was equilibrated with 95% O_2–5% CO_2. The partial pressure of oxygen (P_{O_2}) of the oxygenated Tyrode solution, measured by a blood gas analyser (ABL 5500, Radiometer Copenhagen, Denmark), was 862 ± 9 mmHg. After a stabilization period of 15–30 min, hearts were exposed to a substrate-free hypoxic Tyrode solution (hypoxia). It had the same composition as given above, except that it contained no glucose and was gassed with 95% N_2–5% CO_2, resulting in a P_{O_2} of 36 ± 1 mmHg. The temperature of these solutions was maintained at 36–37°C. After 10 min of hypoxia, the hearts were reoxygenated by changing the perfusate to the normal oxygenated Tyrode solution for 10 min. Right atrial (RA) and right ventricular (RV) electrograms were continuously recorded with monopolar electrodes attached to the walls of RA and RV. A reference electrode was attached to the aorta of the isolated heart. Electrograms were amplified by a bioelectric amplifier (AVB-10, Nihon Kohden, Tokyo, Japan), digitalized with an analog-to-digital converter and stored on a disk of a personal computer with a data acquisition system (PowerLab 4SP, ADInstruments, Castle Hill, Australia). The experimental data were analysed using Chart software (version 5; ADInstruments).

Cell isolation

Single SAN cells were isolated according to the method previously described (Verheijck *et al.* 1998; Lei *et al.* 2004). Briefly, isolated hearts were perfused with an oxygenated Hepes-buffered Tyrode solution at 36°C for 5–10 min to wash out the blood and stabilize the sinus rate. After stabilization, each heart was perfused with low enzyme-containing (1–2 U ml^{-1} Type II collagenase, Worthington Biochemical Corporation, New Jersey, USA) normal Tyrode solution for 5–10 min. The right atrium wall was cut off from the heart, and the SAN region, limited by the crista terminalis, the atrial septum and the orifices of the vena cavae, was anatomically isolated. The excised SAN tissue strip containing the primary pacemaking region was incubated for 5 min in the low-Ca^{2+} (5 μM) Tyrode solution at 36°C, treated with collagenase (120–160 U ml^{-1})-containing low-Ca^{2+} Tyrode solution for 45–60 min, and finally washed with and stored in Kraft-Brühe (KB) medium solution for 1–2 h at 4°C. Single SAN cells were gently isolated from the strip by pipetting KB solution just before experiments. Then the cells were transferred to the recording bath and perfused with the normal Tyrode solution at 36°C.

Composition of solutions

The composition of the Hepes-Tyrode solution was (mM): 143 NaCl, 5.4 KCl, 1.8 $CaCl_2$, 0.5 $MgCl_2$, 0.33 NaH_2PO_4, 5.5 glucose and 10 Hepes-NaOH buffer (pH 7.4). KB solution contained (mM): 70 KOH, 50 L-glutamic acid, 40 KCl, 20 taurine, 20 KH_2PO_4, 3 $MgCl_2$, 10 glucose, 1 EGTA and 10 Hepes-KOH buffer (pH 7.4 adjusted with KOH). The pipette solution for ruptured patch experiments contained (mM): 110 KOH, 110 L-aspartic acid, 20 KCl, 1 $MgCl_2$, 1.41 $CaCl_2$, 1 K_2-ATP, 1 potassium phosphocreatine, 10 EGTA and 5 Hepes-KOH buffer (pH 7.4 adjusted with KOH), and that for nystatin-perforated patch experiments contained (mM): 110 KOH, 110 L-aspartic acid, 20 KCl, 1 $MgCl_2$, 1 $CaCl_2$, 0.1 EGTA and 5 Hepes-KOH buffer (pH 7.4 adjusted with KOH). Nystatin (Wako Pure Chemicals, Osaka, Japan) was first dissolved in dimethyl sulfoxide (DMSO; Sigma-Aldrich Japan, Tokyo, Japan) and then added to the pipette solution at a concentration of 300–500 μg ml^{-1} just prior to use; the final concentration of DMSO was less than 0.1%.

Electrophysiology

Single SAN cells were identified by their characteristic morphology, a long and slender shape with faint

sarcomere striations, and spontaneous activity, as previously described (Verheijck *et al.* 1998; Boyett *et al.* 2000; Cho *et al.* 2003). The whole-cell patch-clamp technique was used for the electrical recordings from single SAN cells. A patch-clamp amplifier (CEZ-2400, Nihon Kohden, Tokyo, Japan) was used for current- and voltage-clamp experiments. Pipette electrodes (resistance 2–6 MΩ) were made by using a Narishige pipette puller (PB-7, Narishige Scientific Instruments Laboratory, Tokyo, Japan). After the gigaohm seal between tip and cell membrane was formed, we ruptured the patch membrane to form the whole-cell patch configuration. In the current-clamp mode, spontaneous action potentials were constantly recorded from pacemaker cells. In the voltage-clamp mode, a ramp-pulse protocol was used to record the quasi-steady-state membrane current at the interval of 15 s. The membrane potential was held at −40 mV and depolarized to +50 mV in 1.0 s. It was then repolarized or hyperpolarized to −100 mV in 2.5 s, during which time the change in the membrane current was automatically plotted against the membrane potential. Spontaneous action potentials and whole-cell membrane currents were also recorded by nystatin-perforated patch configuration, as previously described (Sakamoto *et al.* 1998). After the gigaohm seal, negative pressure was released to await gradual opening of nystatin-induced pores. The experiments were performed at 36°C. The current signals were filtered at 10 kHz and digitalized at 1 or 2 kHz by using an A/D converter (Digidata 1322A, Axon Instruments Inc., Union City, CA, USA). All data were stored on a computer for later analysis with pCLAMP9 software (Axon Instruments).

Cytosolic Ca^{2+} concentration measurement

The cytosolic Ca^{2+} concentration ($[Ca^{2+}]_i$) was measured as previously described (Yao *et al.* 1998; Matsuura *et al.* 2004). Single SA node cells were incubated in Hepes-Tyrode (loading) solution containing 1 μM fluo-3 acetoxymethyl ester (fluo-3 AM; Molecular Probes, OR, USA) at 36°C in the dark for 30 min. The loading solution was prepared by diluting a 10 μM stock solution, which contained 90% FBS, 10% DMSO and 0.45% Pluronic F127 (Molecular Probes). Fluo-3-loaded SAN cells were perfused with Hepes-buffered Tyrode solution at 36°C. Fluo-3 was excited at 480 nm, and emitted fluorescence was recorded at 520 nm by a photomultiplier tube (AIM-10, InterMedical Co, Aichi, Japan). Although 2,4-dinitrophenol can reportedly cause an increase in flavoprotein autofluorescence excited at 480 nm (Sato *et al.* 1998), it was confirmed that the autofluorescence did not produce any appreciable effects on the fluo-3 fluorescence because of the very low intensity of the endogenous fluorescence.

Chemicals

Glibenclamide (Sigma-Aldrich Japan) was dissolved in DMSO as a stock solution of 10 mM, and the final concentration of DMSO in the perfusate was less than 0.1%. Pinacidil (Sigma-Aldrich Japan) was dissolved in 0.1 N HCl as a stock solution of 20 mM. 2,4-Dinitrophenol (Wako Pure Chemicals) was directly dissolved in Tyrode solution.

Statistics

All data are presented as mean ± S.E.M. The number of experiments is shown as *n*. Statistical significance was evaluated by Student's t test for paired or unpaired observations or analysis of variance (ANOVA), where appropriate. Differences with values of $P < 0.05$ were considered to be statistically significant.

Results

SAN function during hypoxia in isolated hearts

Representative electrograms recorded from RA and RV under control conditions (oxygenated solution), hypoxia (hypoxic and glucose-free solution) and after reoxygenation (reintroduction of control oxygenated solution) are shown in Fig. 1*A*. In WT hearts, the spontaneous cycle length (CL) of RA electrograms was gradually prolonged during hypoxia and recovered to the control levels after 5 min of reoxygenation. Concomitantly, atrioventricular (AV) block developed during hypoxia and disappeared after reoxygenation in WT hearts. However, in Kir6.2 KO hearts, the prolongation of CL observed during hypoxia was not so marked but atrial electrograms disappeared abruptly. AV block also developed in Kir6.2 KO hearts during hypoxia. RA electrograms did not recover after reoxygenation in most of the Kir6.2 KO hearts.

Figure 1*B* summarizes the time course of changes in CL of RA electrograms during hypoxia and reoxygenation in WT and Kir6.2 KO hearts. There was no significant difference in the basal CL between WT (206.5 ± 10.1 ms; $n = 15$) and Kir6.2 KO hearts (197.5 ± 16.5 ms; $n = 15$). During hypoxia, CL of RA electrograms in WT hearts was gradually and significantly prolonged to 324.2 ± 23.4 ms at 2 min ($n = 13$, $P < 0.05$ *versus* 0 min) and to 613.2 ± 84.3 ms at 5 min ($n = 13$, $P < 0.001$ *versus* 0 min) of hypoxia although RA electrograms were invisible at these time points in 2 of 15 WT hearts. In Kir6.2 KO hearts, CL was slightly but significantly prolonged to 274.1 ± 34.5 ms ($n = 15$, $P < 0.05$ *versus* 0 min) at 2 min hypoxia. At 5 min of hypoxia RA electrograms were invisible in 4 Kir6.2 KO hearts and CL of RA electrograms in other 11 Kir6.2 KO hearts was insignificantly prolonged

to 265.3 ± 31.5 ms (*P* is not significant (NS) *versus* 0 min). After 5 min of reoxygenation, CL was almost completely recovered in all WT hearts (236.2 ± 21.9 ms; $n = 15$, $P < 0.05$ *versus* 10 min of hypoxia, NS *versus* 0 min). However, in only 6 of 15 Kir6.2 KO hearts RA electrograms could be recorded after 5 min of reoxygenation and the CL was 208.5 ± 25.5 ms ($n = 6$, P = NS *versus* 10 min of hypoxia).

Effect of K_{ATP} channel opener on action potentials of SAN cells

We next examined the effect of pinacidil, a K^+ channel opener, on spontaneous pacemaker activity of enzymatically isolated SAN cells in the current-clamp mode of the ruptured patch clamp techniques. Representative recordings of spontaneous action

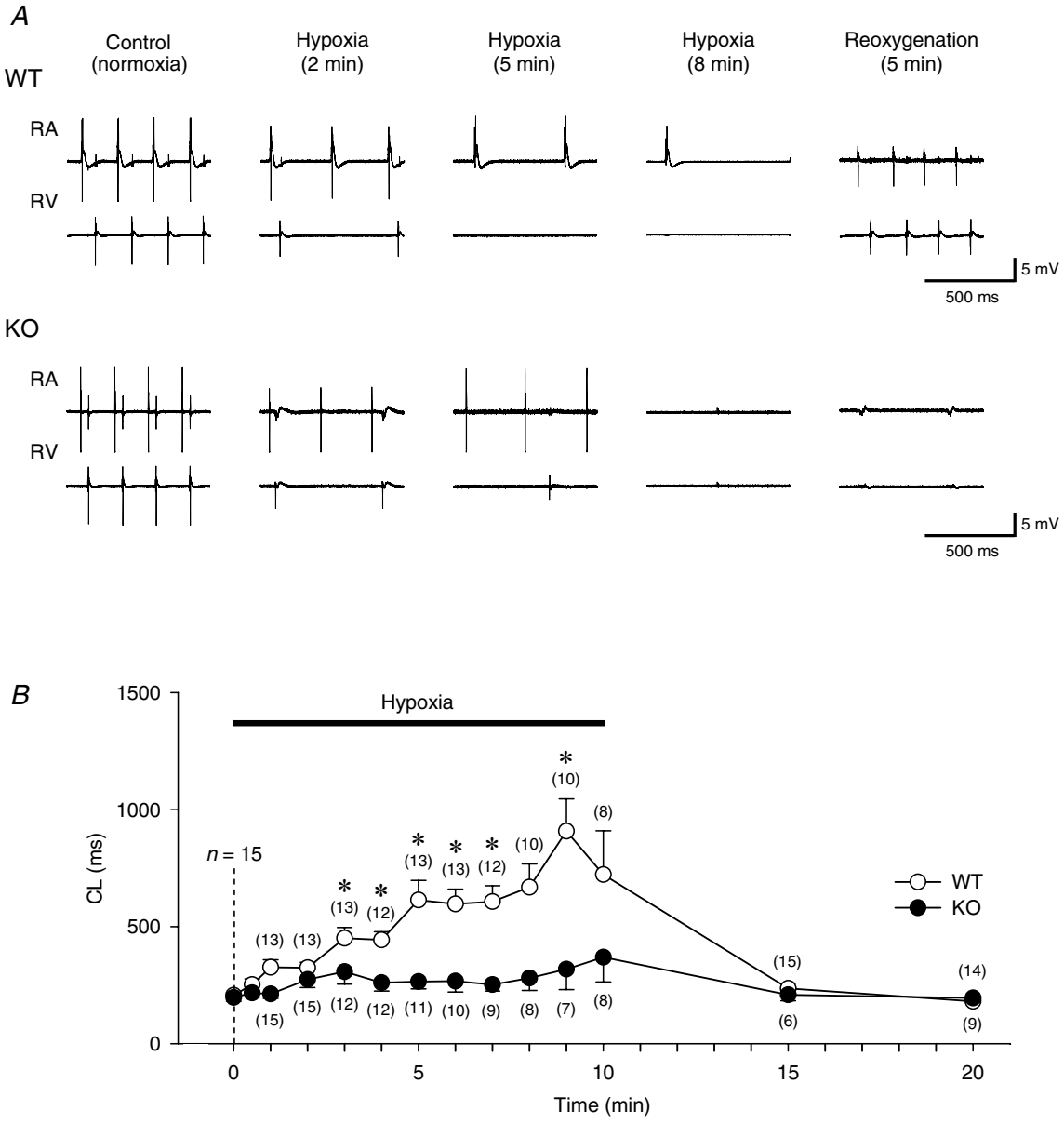

Figure 1. Effects of hypoxia on sinus cycle length (CL) of wild-type (WT) and Kir6.2-deficient (KO) mouse hearts

A, representative traces of the electrograms recorded from right atrium (RA) and right ventricle (RV) during normoxia (control), hypoxia (2 and 5 min) and after 5 min of reoxygenation. *B*, time course changes of the CL during hypoxia and after reoxygenation in WT ($n = 15$, ○) and Kir6.2 KO ($n = 15$, ●) hearts. The number of hearts from which RA electrograms could be recorded and the CL measured are shown in parentheses. Values are expressed as means ± S.E.M. *$P < 0.001$ *versus* 0 min.

potentials of WT SAN cells before (Cont) and after pinacidil (100 μM)-treatment (PIN) are shown in Fig. 2*A*. Pinacidil significantly prolonged CL of spontaneous action potentials from 409.7 ± 56.1 to 605.4 ± 108.4 ms ($n = 6$, $P < 0.05$) in WT SAN cells, as shown in Fig. 2*B*. The increasing effect of pinacidil on CL was partially reversed by the addition of glibenclamide (1 μM, PIN + GLB). In contrast, CL of SAN cells of Kir6.2 KO mice was affected by neither pinacidil alone nor co-administration of pinacidil and glibenclamide. Figure 2*C* summarizes the changes of the slope of the diastolic depolarization (SDD) after administration of

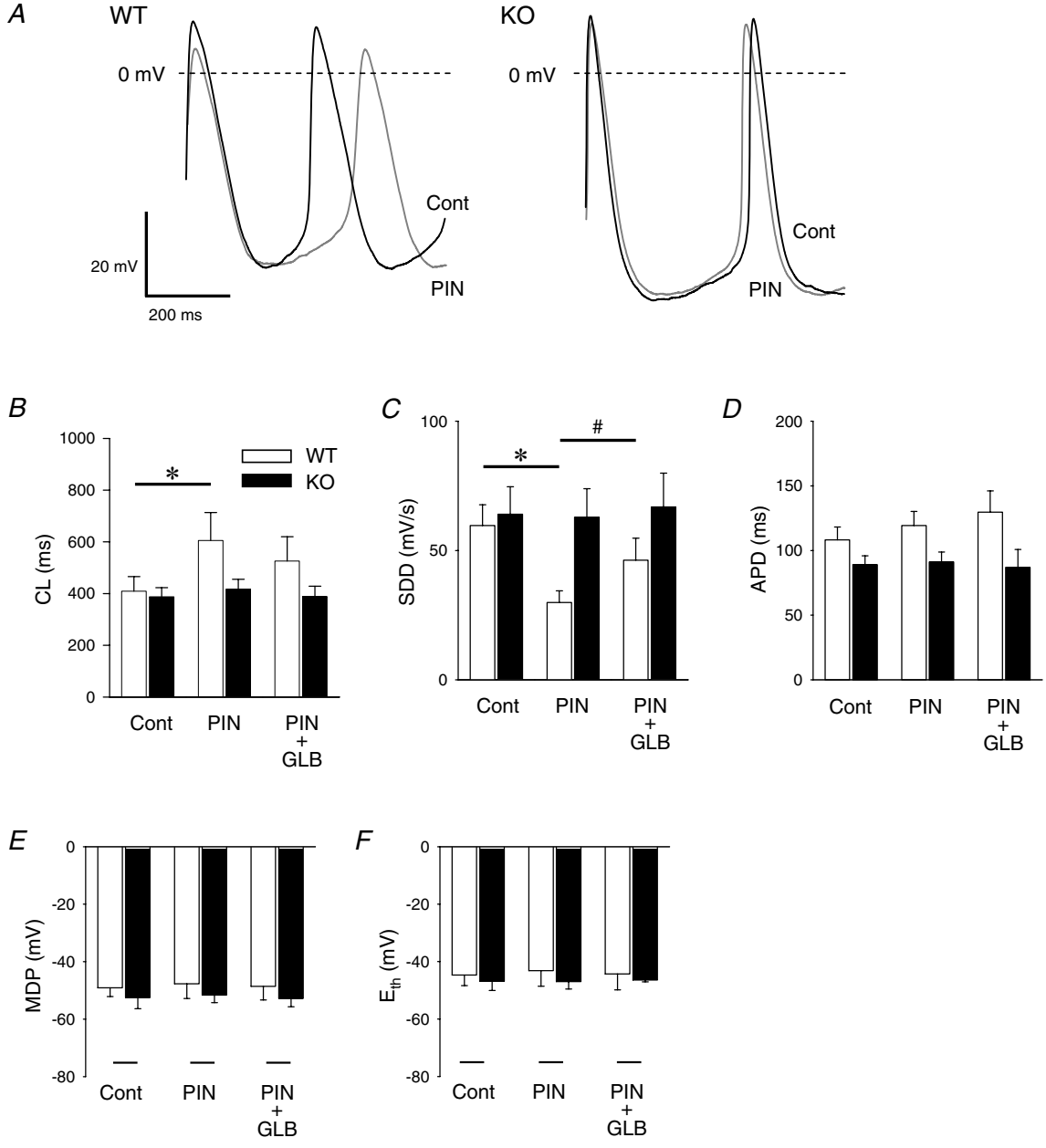

Figure 2. Effects of pinacidil on the action potential recorded from SAN cells of wild-type (WT) and Kir6.2-deficient (KO) mice

A, representative traces of action potentials recorded from WT and Kir6.2 KO SAN cells in control conditions (black lines, Cont) and after 100 μM pinacidil (grey lines, PIN). Action potential parameters of WT (open columns) and Kir6.2 KO (filled columns) SAN cells in control conditions, after 100 μM pinacidil (PIN) and after addition of 1 μM glibenclamide (PIN + GLB) are summarized. The cycle length of spontaneous action potentials (CL, *B*), the slope of the diastolic depolarization (SDD, *C*), the action potential duration at 80% repolarization (APD_{80}, *D*), the maximum diastolic potential (MDP, *E*) and the voltage threshold of the action potential upstroke (E_{th}, *F*) are shown. Values are expressed as means ± S.E.M. $^*P < 0.05$ *versus* Cont, #$P < 0.05$ *versus* PIN.

these drugs in WT and Kir6.2 KO SAN cells. The decreased spontaneous pacemaker activity in WT SAN cells after pinacidil was accompanied by the decrease of SDD from 59.6 ± 8.1 to 29.9 ± 4.5 mV s^{-1} ($n = 6$, $P < 0.01$). The pinacidil-induced decrease of SDD was antagonized by addition of glibenclamide (46.2 ± 8.5 mV s^{-1}; $n = 4$, $P < 0.05$ *versus* pinacidil alone). However, the change of SDD after pinacidil was not observed in Kir6.2 KO SAN cells.

There were also no significant differences in the basal action potential parameters between WT and Kir6.2 KO SAN cells. These drugs produced no significant effects on the other action potential parameters such as the action potential duration at 80% repolarization level (APD_{80}, Fig. 2*D*), the maximum diastolic potential (MDP, Fig. 2*E*) and the voltage threshold of the action potential upstroke (E_{th}, Fig. 2*F*) in WT as well as Kir6.2 KO SAN cells.

K_{ATP} current in SAN cells

Whole-cell membrane currents were recorded from WT and Kir6.2 KO SAN cells using a ramp-pulse protocol of the ruptured patch clamp. Effects of pinacidil (100 μM) on the quasi-steady-state membrane current were examined in WT and Kir6.2 KO SAN cells. Pinacidil increased an outward current, which was sensitive to 1 μM glibenclamide, in WT SAN cells but not in Kir6.2 KO SAN cells (Fig. 3*A*). There was no significant difference

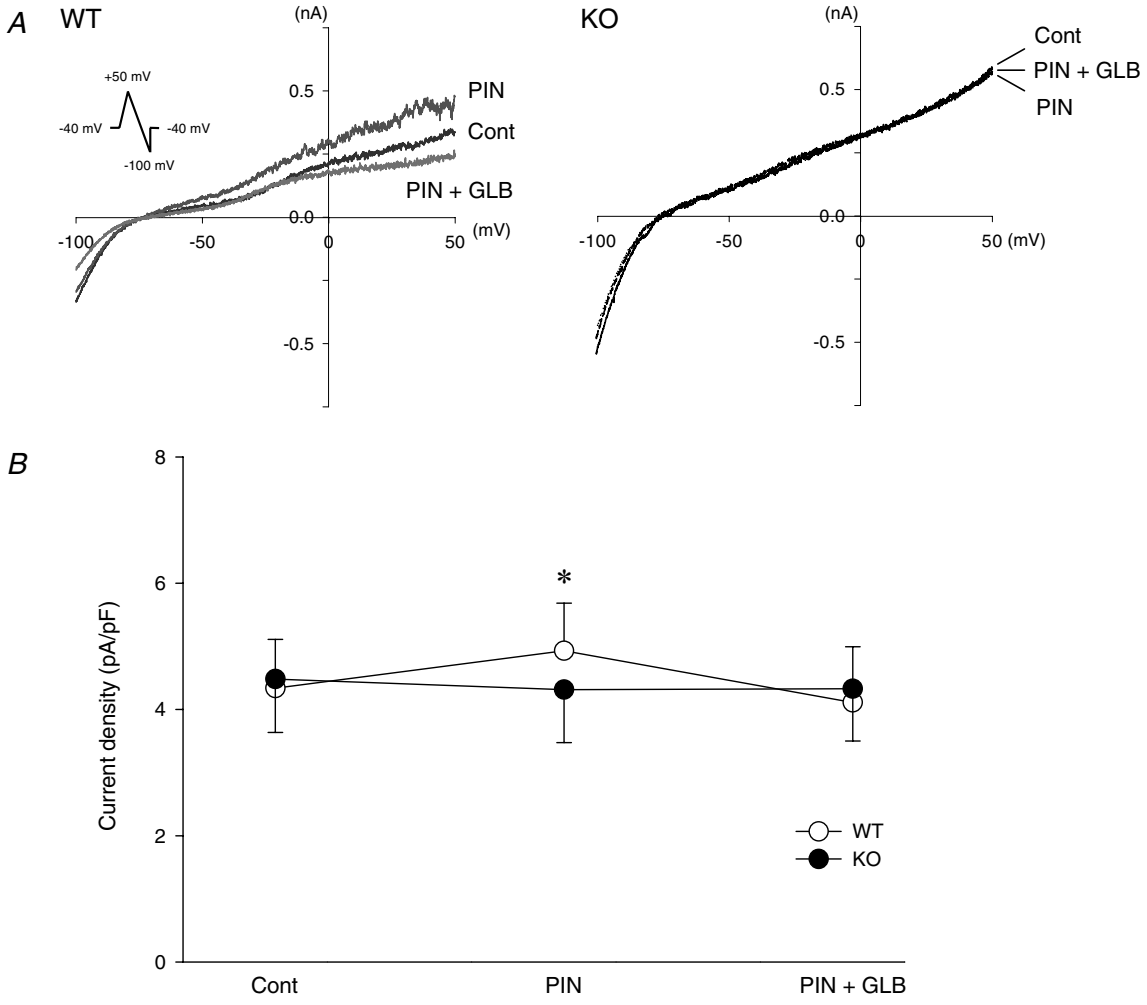

Figure 3. Effects of pinacidil on the whole-cell membrane currents in SAN cells of wild-type (WT) and Kir6.2-deficient (KO) mice

A, representative traces of quasi-steady-state membrane currents elicited by a ramp-pulse protocol (shown in the inset) in control conditions (black, Cont), after 100 μM pinacidil (dark grey, PIN) and after addition of 1 μM glibenclamide (grey, PIN + GLB) are shown. *B*, PIN-induced current densities at the membrane potential of 0 mV in WT ($n = 7$, ○) and Kir6.2 KO SAN cells ($n = 7$, ●) in control conditions (Cont), after 100 μM pinacidil (PIN) and after addition of 1 μM glibenclamide (PIN + GLB) are summarized. Values are expressed as means ± S.E.M. *$P < 0.05$ *versus* Cont.

in the basal value of the outward current density at 0 mV between WT and Kir6.2 KO SAN cells. In WT SAN cells the density of the outward current at 0 mV was increased from 4.3 ± 0.8 to 4.9 ± 0.8 pA pF^{-1} ($n = 7$, $P < 0.05$) after pinacidil and returned to 4.1 ± 0.9 pA pF^{-1} after addition of glibenclamide (Fig. 3*B*). In contrast, pinacidil hardly affected the density of the outward current at 0 mV (from 4.5 ± 0.8 to 4.3 ± 0.8 pA pF^{-1}; $n = 7$, $P =$ NS) in Kir6.2 KO SAN cells (Fig. 3*B*). Addition of glibenclamide also did not change the outward current. Thus, pinacidil could induce a glibenclamide-sensitive outward current only in WT SAN cells.

Pacemaker activity and membrane currents of SAN cells during metabolic inhibition

Metabolic inhibition was produced by exposure of WT and Kir6.2 KO SAN cells to the glucose-free and 2,4-dinitrophenol (DNP, 50 μM)-containing Tyrode solution. Figure 4*A* shows representative traces of spontaneous action potentials recorded from WT and Kir6.2 KO SAN cells by nystatin-perforated patch configuration before (Cont) and after metabolic inhibition (DNP). In Kir6.2 KO SAN cells, MDP was gradually depolarized with the reduction of action potential amplitude during metabolic inhibition. MDP of Kir6.2 KO SAN cells was significantly decreased from -52.6 ± 3.0 mV (Cont) to -44.7 ± 3.6 mV at the time point just prior to the end of spontaneous activity during metabolic inhibition ($n = 5$, $P < 0.05$). Such a gradual decrease of MDP during metabolic inhibition was hardly observed in WT SAN cells. MDP of WT SAN cells was changed from -50.2 ± 4.0 mV (Cont) to -50.4 ± 4.3 mV at the time point just prior to the end of spontaneous activity during metabolic inhibition ($n = 6$, $P =$ NS). Application of DNP markedly decreased SDD in WT SAN cells but not in Kir6.2 KO SAN cells. Changes of CL in WT and Kir6.2 KO SAN cells during metabolic inhibition until disappearance of spontaneous action potentials are summarized in Fig. 4*B*. The CL of SAN action potentials in WT was significantly prolonged from 292.2 ± 38.2 to 585.4 ± 91.2 ms ($n = 6$, $P < 0.05$) just prior to the SAN cell arrest or 5 min after DNP application. However, in Kir6.2 KO SAN cells the CL was changed from 284.6 ± 50.1 to 293.6 ± 51.6 ms ($n = 5$, $P =$ NS) just prior to the disappearance of action potentials (Fig. 4*B* and *C*). Changes of SDD and APD_{80} after metabolic inhibition in WT and Kir6.2 KO SAN cells are summarized in Fig. 4*C*. At the time point just prior to the disappearance of action potentials or at 5 min of DNP treatment, SDD was significantly decreased from 91.1 ± 11.9 to 32.2 ± 6.5 mV s^{-1} ($n = 6$, $P < 0.05$) in WT SAN cells (Fig. 4*D*). However, no significant change of SDD was observed in Kir6.2 KO SAN cells. Metabolic inhibition produced no significant changes in APD_{80} in WT or Kir6.2 KO SAN cells (Fig. 4*E*).

Effects of metabolic inhibition on the membrane currents of WT and Kir6.2 KO SAN cells were also examined using the nystatin-perforated patch clamp method. In WT SAN cells the density at 0 mV of the quasi-steady-state membrane current recorded by a ramp-pulse protocol was significantly increased by $33.6 \pm 12.2\%$ of the control ($n = 5$, $P < 0.05$) at 2 min after metabolic inhibition. In Kir6.2 KO SAN cells, however, the density at 0 mV of the quasi-steady-state current after 2 min metabolic inhibition was $94.2 \pm 3.6\%$ of the control ($n = 3$, $P =$ NS). Effects of metabolic inhibition on the L-type Ca^{2+} current ($I_{Ca\text{-}L}$) were also examined in WT and Kir6.2 KO SAN cells. The $I_{Ca\text{-}L}$ was evoked by a 300 ms depolarizing pulse to 0 mV from a holding potential of -40 mV at a frequency of once every 15 s. At 2 min after metabolic inhibition the amplitude of $I_{Ca\text{-}L}$, measured as the difference between the peak current and the steady-state current at the end of test pulse, was decreased to $62.3 \pm 7.1\%$ ($n = 4$, $P < 0.05$) and $66.6 \pm 8.7\%$ ($n = 4$, $P < 0.05$) of the control in WT and Kir6.2 KO SAN cells, respectively. Thus, after metabolic inhibition the outward current was significantly increased in WT but not in Kir6.2 KO SAN cells although the $I_{Ca\text{-}L}$ was decreased to a similar extent in both types of SAN cells.

$[Ca^{2+}]_i$ changes in SAN cells during metabolic inhibition

We measured $[Ca^{2+}]_i$ by loading SAN cells with fluo-3. A spontaneous Ca^{2+}-transient was observed in both WT and Kir6.2 KO SAN cells under control conditions (Fig. 5*A*). After the introduction of DNP-containing glucose-free solution (metabolic inhibition) the spontaneous Ca^{2+} transient of WT SAN cells disappeared and diastolic $[Ca^{2+}]_i$ was slightly decreased when spontaneous activity was stopped. However, in Kir6.2 KO SAN cells the spontaneous Ca^{2+} transient did not quite disappear and the diastolic $[Ca^{2+}]_i$ gradually increased with a decreased amplitude of the Ca^{2+} transient during metabolic inhibition.

Figure 5*B* summarizes the time course of changes in the peak and diastolic $[Ca^{2+}]_i$ during metabolic inhibition. In the control condition the amplitude of the Ca^{2+} transient was 1.56 ± 0.10 ($n = 5$) and 1.33 ± 0.05 F/F_0 ($n = 5$) in WT and Kir6.2 KO SAN cells, respectively, and there was no significant difference between these values. In WT SAN cells, diastolic $[Ca^{2+}]_i$ (F/F_0) was decreased to $88 \pm 3\%$ and $83 \pm 6\%$ of the control ($n = 5$) after 1.5 and 2.5 min of metabolic inhibition, respectively. However, in Kir6.2 KO SAN cells diastolic $[Ca^{2+}]_i$ was gradually and continuously increased to $104 \pm 3\%$ and $115 \pm 9\%$ of the control ($n = 5$) after 1.5 and 2.5 min of metabolic

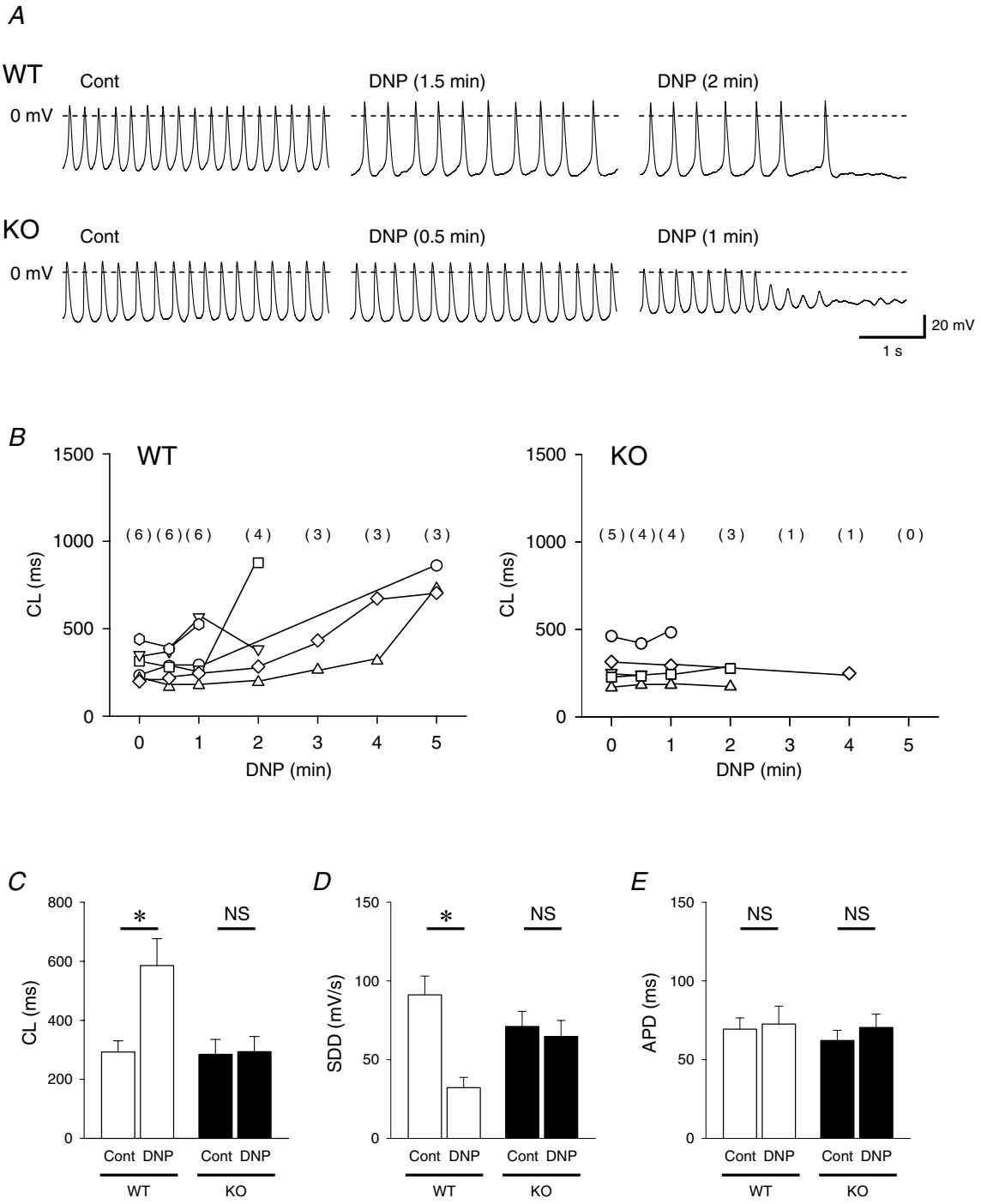

Figure 4. Action potential changes of SAN cells of wild-type (WT) and Kir6.2-deficient (KO) mice during metabolic inhibition

A, representative changes in action potentials recorded from WT and Kir6.2 KO SAN cells in nystatin-perforated patch configuration before (Cont) and after metabolic inhibition. The SAN cells were exposed to a glucose-free, DNP (50 μM 2,4-dinitrophenol)-containing solution. Action potentials before (Cont), after metabolic inhibition and just prior to the end of spontaneous activity are shown. *B*, time course of the changes in CL of WT and Kir6.2 KO SAN cells. The number of cells with amplitudes more than 50% of control in both groups are indicated in parentheses. *C–E*, changes in cycle length (CL) of spontaneous action potentials, slope of the diastolic depolarization (SDD), and action potential duration at 80% repolarization (APD) before and after metabolic inhibition (DNP) in WT and Kir6.2 KO SAN cells. Values are expressed as means ± S.E.M. $^*P < 0.05$ *versus* Cont.

inhibition, respectively. These changes in diastolic $[Ca^{2+}]_i$ during metabolic inhibition were significantly different between WT and Kir6.2 KO SAN cells.

Discussion

Using mice with homozygous knockout of the Kir6.2 or Kir6.1 gene, previous studies from our laboratory have indicated that Kir6.2 forms the pore region of ventricular K_{ATP} channels whereas Kir6.1 forms that of vascular K_{ATP} channels (Suzuki *et al.* 2001; Miki *et al.* 2002). In addition, it has been indicated that Kir6.2 is essential for the K_{ATP} channel function in mouse atrial cells (Saegusa *et al.* 2005). Although several studies have indicated the presence of K_{ATP} channels in the sinoatrial node (Han *et al.* 1996; Marionneau *et al.* 2005), the pathophysiological role is not well defined. We tried to determine the role of SAN cells using Kir6.2-null mice.

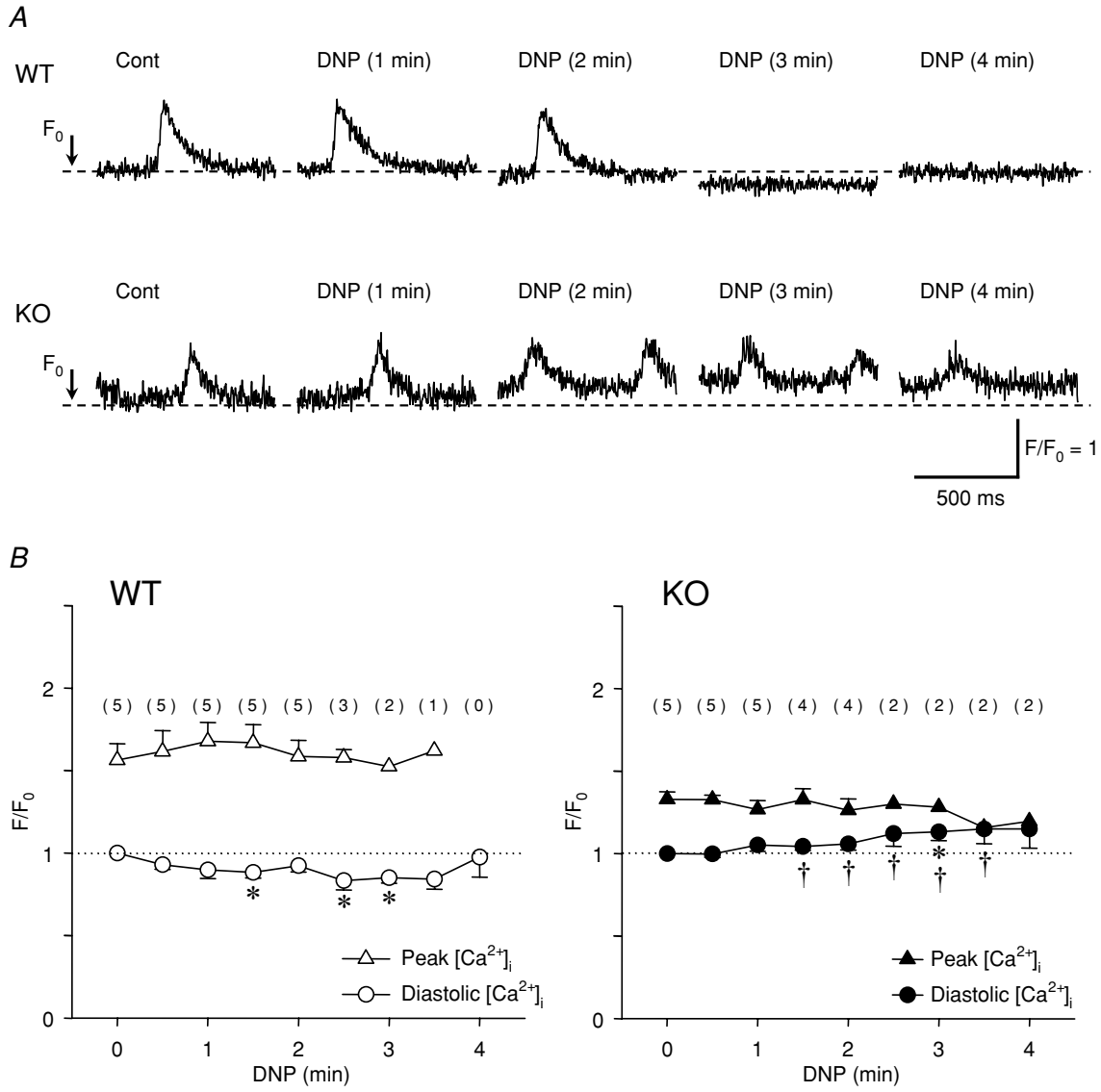

Figure 5. Changes in $[Ca^{2+}]_i$ during metabolic inhibition in wild-type (WT) and Kir6.2-deficient (KO) SAN cells

A, representative changes in Ca^{2+} transient during metabolic inhibition in WT and Kir6.2 KO SAN cells. Note that the diastolic $[Ca^{2+}]_i$ in WT SAN cells was slightly decreased after the disappearance of the Ca^{2+} transient whereas the diastolic $[Ca^{2+}]_i$ was gradually increased without the disappearance of the Ca^{2+} transient in Kir6.2 KO SAN cells. *B*, time course changes in the peak (triangles) and diastolic $[Ca^{2+}]_i$ (circles) during metabolic inhibition in WT (open symbols, $n = 5$) and Kir6.2 KO SAN cells (filled symbols, $n = 5$). The numbers of cells in which the Ca^{2+} transient was detected and the peak $[Ca^{2+}]_i$ could be measured are indicated in parentheses. Values are expressed as means ± S.E.M. $^*P < 0.05$ *versus* 0 min, †$P < 0.05$ *versus* WT in diastolic $[Ca^{2+}]_i$ values.

In the present study the K^+ channel opener pinacidil activated a glibenclamide-sensitive outward current in WT SAN cells but not in Kir6.2 KO SAN cells. Therefore, Kir6.2 forms the pore region of K_{ATP} channels of mouse SAN cells, which is similar to K_{ATP} channels of atrial and ventricular cells (Suzuki *et al.* 2001; Saegusa *et al.* 2005). However, the density of pinacidil-induced outward current in mouse SAN cells ($\sim$0.6 pA pF^{-1}) was much lower than in mouse ventricular cells ($\sim$25 pA pF^{-1}) (Suzuki *et al.* 2001) and that observed in atrial cells ($\sim$7.5 pA pF^{-1}) during metabolic inhibition (Saegusa *et al.* 2005). A recent study by Marionneau *et al.* (2005) has indicated that mRNA expression of Kir6.2 and SUR2 in SAN is lower than that in atrial and ventricular myocardium of the mouse heart. Pinacidil prolonged the cycle length of WT SAN cells by decreasing SDD, which was antagonized by the addition of glibenclamide. However, reduction of spontaneous activity of WT SAN cells after pinacidil was not accompanied by changes of other action potential parameters such as APD and MDP. It was reported that in rabbit SAN cells pinacidil at a concentration of 50 μM hyperpolarized MDP by $\sim$10 mV and decreased spontaneous pacemaker rate (Han *et al.* 1996), which is apparently inconsistent with the findings of this study. The different responses to pinacidil between mouse and rabbit SAN cells might be ascribed to different densities of the K_{ATP} current in these cells. In this study pinacidil at 100 μM increased the quasi-steady-state outward current at 0 mV by approximately 15% in WT mouse SAN cells (Fig. 3). In our preliminary experiments using rabbit SAN cells pinacidil at 30 and 100 μM increased the quasi-steady-state current at 0 mV by approximately 300% and 600%, respectively, which was antagonized by 1 μM glibenclamide (data not shown).

Metabolic inhibition of 2 min also increased the outward current by about 30% in WT SAN cells but not in Kir6.2 KO SAN cells. However, metabolic inhibition may affect other ionic currents such as L- and T-type Ca^{2+} current ($I_{Ca\text{-}L}$ and $I_{Ca\text{-}T}$), and hyperpolarization-activated inward current (I_f), thereby inhibiting SAN automaticity. In fact metabolic inhibition of 2 min decreased $I_{Ca\text{-}L}$ by 30–40% in both WT and Kir6.2 KO SAN cells. Since the decreases of $I_{Ca\text{-}L}$ after metabolic inhibition were of similar magnitude in these cells, activation of K_{ATP} channels might be responsible for a more marked decrease of SAN automaticity in WT SAN cells.

It was reported that the activation of muscarinic acetylcholine receptor-operated K^+ (K_{ACh}) current by a low concentration of acetylcholine produced the reduction of spontaneous automaticity which was associated with a decrease in SDD but no change in APD or MDP (DiFrancesco *et al.* 1989). We also examined the effect of a low concentration (30 nM) of carbachol, a muscarinic agonist, on the pacemaker activity in SAN cells of WT mouse, and found that the carbachol-induced prolongation of CL was associated with only the decrease in SDD (data not shown). Muscarinic receptor stimulation may indirectly inhibit $I_{Ca\text{-}L}$ and I_f by decreasing intracellular cAMP and modulate the action potential configuration of SAN tissue *in situ*. Therefore, similarity of SAN action potential changes during K_{ATP} and K_{ACh} channel activation may not guarantee the hypothesis. However, it may provide a piece of evidence for the concept that mild activation of inward rectifier K^+ channels may inhibit SAN automaticity by decreasing SDD.

When Langendorff-perfused hearts of WT mice were exposed to hypoxic and glucose-free conditions, the CL of RA electrograms, an indirect index of SAN automaticity, was prolonged more markedly compared to the hypoxia-induced CL prolongation observed in Kir6.2 KO hearts. Metabolic inhibition also prolonged the CL of spontaneous action potentials with decrease of SDD in WT SAN cells. The CL prolongation of spontaneous action potentials in WT SAN cells was more marked than that observed in Kir6.2 KO SAN cells during metabolic inhibition. Therefore, activation of sarcolemmal K_{ATP} channels might be at least in part involved in the sinus slowing or sinus arrest during hypoxia or metabolic inhibition. However, even in isolated hearts and SAN cells of Kir6.2 KO mice CL of spontaneous automaticity was slightly prolonged during hypoxia or metabolic inhibition. Therefore, changes in other ionic current(s) might also contribute to the decreased SAN automaticity. A decrease in intracellular ATP during metabolic inhibition might result in a decrease in cAMP, thereby decreasing $I_{Ca\text{-}L}$, $I_{Ca\text{-}T}$ and I_f. It has been reported that these inward currents can be modulated by intracellular cAMP and cAMP-dependent protein kinase A (Kaupp & Seifert, 2001; Qu *et al.* 2005; Kim *et al.* 2006). In addition, an increase in $[Ca^{2+}]_i$ during metabolic inhibition might lead to decreases of $I_{Ca\text{-}L}$ and $I_{Ca\text{-}T}$. In fact, metabolic inhibition reduced $I_{Ca\text{-}L}$ to a similar extent in both WT and Kir6.2 KO SAN cells although it activated an outward current in WT but not Kir6.2 KO SAN cells. Therefore, changes in other ionic currents including $I_{Ca\text{-}L}$ may also be involved in sinus slowing during metabolic inhibition or hyoxia.

Although RA electrograms, probably reflecting SAN automaticity, recovered after reoxygenation in all WT hearts, the recovery was worse in Kir6.2 KO hearts. These results suggest that an increase in $[Ca^{2+}]_i$ during hypoxia might be involved in impaired recovery of SAN function in Kir6.2 KO hearts. In WT SAN cells metabolic inhibition suppressed spontaneous firing by decreasing SDD. However, in Kir6.2 KO SAN cells metabolic inhibition produced less marked CL prolongation without a significant change in SDD and slight decrease of MDP. Decrease of spontaneous firing due to activation of K_{ATP} channels might decrease Ca^{2+} influx through the L-type Ca^{2+} channel in WT SAN cells. Maintenance of MDP resulting from K_{ATP} channel activation might keep the

efficient Ca^{2+} extrusion through the Na^+–Ca^{2+} exchange system in WT SAN cells. In Kir6.2 KO SAN cells, a less marked decrease of spontaneous firing and slight decrease in MDP might result in an increase in diastolic $[Ca^{2+}]_i$. An increase in $[Ca^{2+}]_i$ during hypoxia might lead to SAN dysfunction. Similarly activation of sarcolemmal K_{ATP} channels can prevent hypoxia/reoxygenation-induced Ca^{2+} overload and improve post-hypoxic cardiac function with reduction in abnormal diastolic Ca^{2+} homeostasis in ventricular myocardium (Baczkó *et al.* 2004, 2005). A previous study from our laboratory has indicated that sarcolemmal K_{ATP} channels are essential for the protection of the ischaemic myocardium (Suzuki *et al.* 2002). It has also been reported that an increase in $[Ca^{2+}]_i$ can lead to the reduction of gap junction conductance and conduction disturbance during hypoxia (Dhein, 1998). Therefore, sarcolemmal K_{ATP} channels are important for the protection of myocardium, the preservation of contractile function and the function of the cardiac conduction system including SAN during metabolic inhibition.

In summary, the present study using Kir6.2-deficient mice has indicated that activation of sarcolemmal K_{ATP} channels in SAN cells contributes to the regulation of SAN automaticity during hypoxia. The SAN slowing resulting from the activation of K_{ATP} channels may be important for the preservation of SAN function during hypoxia or ischaemia.

References

Baczkó I, Giles WR & Light PE (2004). Pharmacological activation of plasma-membrane K_{ATP} channels reduces reoxygenation-induced Ca^{2+} overload in cardiac myocytes via modulation of the diastolic membrane potential. *Br J Pharmacol* **141**, 1059–1067.

Baczkó I, Jones L, McGuigan CF, Manning Fox JE, Gandhi M, Giles WR, Clanachan AS & Light PE (2005). Plasma membrane K_{ATP} channel-mediated cardioprotection involves posthypoxic reductions in calcium overload and contractile dysfunction: mechanistic insights into cardioplegia. *FASEB J* **19**, 980–982.

Boyett MR, Honjo H & Kodama I (2000). The sinoatrial node, a heterogeneous pacemaker structure. *Cardiovasc Res* **47**, 658–687.

Cho HS, Takano M & Noma A (2003). The electrophysiological properties of spontaneously beating pacemaker cells isolated from mouse sinoatrial node. *J Physiol* **550**, 169–180.

Dhein S (1998). Gap junction channels in the cardiovascular system: pharmacological and physiological modulation. *Trends Pharmacol Sci* **19**, 229–241.

DiFrancesco D, Ducouret P & Robinson RB (1989). Muscarinic modulation of cardiac rate at low acetylcholine concentrations. *Science* **243**, 669–671.

Han X, Light PE, Giles WR & French RJ (1996). Identification and properties of an ATP-sensitive K^+ current in rabbit sino-atrial node pacemaker cells. *J Physiol* **490**, 337–350.

Hernandez-Benito MJ, Macianskiene R, Sipido KR, Flameng W & Mubagwa K (2001). Suppression of transient outward potassium currents in mouse ventricular myocytes by imidazole antimycotics and by glybenclamide. *J Pharmacol Exp Ther* **298**, 598–606.

Irisawa H, Brown HF & Giles W (1993). Cardiac pacemaking in the sinoatrial node. *Physiol Rev* **73**, 197–227.

Kaupp UB & Seifert R (2001). Molecular diversity of pacemaker ion channels. *Annu Rev Physiol* **63**, 235–257.

Keith A & Flack M (1907). The form and nature of the muscular connections between the primary divisions of the vertebrate heart. *J Anat Physiol* **41**, 172–189.

Kim JA, Park JY, Kang HW, Huh SU, Jeong SW & Lee JH (2006). Augmentation of $Ca_V3.2$ T-type calcium channel activity by cAMP-dependent protein kinase A. *J Pharmacol Exp Ther* **318**, 230–237.

Kodama I, Nikmaram MR, Boyett MR, Suzuki R, Honjo H & Owen JM (1997). Regional differences in the role of the Ca^{2+} and Na^+ currents in pacemaker activity in the sinoatrial node. *Am J Physiol Heart Circ Physiol* **272**, H2793–H2806.

Lee SY & Lee CO (2005). Inhibition of Na^+-K^+ pump and L-type Ca^{2+} channel by glibenclamide in guinea pig ventricular myocytes. *J Pharmacol Exp Ther* **312**, 61–68.

Lei M, Jones SA, Liu J, Lancaster MK, Fung SS, Dobrzynski H, Camelliti P, Maier SK, Noble D & Boyett MR (2004). Requirement of neuronal- and cardiac-type sodium channels for murine sinoatrial node pacemaking. *J Physiol* **559**, 835–848.

Mangoni ME, Traboulsie A, Leoni AL, Couette B, Marger L, Le Quang K, Kupfer E, Cohen-Solal A, Vilar J, Shin HS, Escande D, Charpentier F, Nargeot J & Lory P (2006). Bradycardia and slowing of the atrioventricular conduction in mice lacking $Ca_V3.1/a_{1G}$ T-type calcium channels. *Circ Res* **98**, 1422–1430.

Marionneau C, Couette B, Liu J, Li H, Mangoni ME, Nargeot J, Lei M, Escande D & Demolombe S (2005). Specific pattern of ionic channel gene expression associated with pacemaker activity in the mouse heart. *J Physiol* **562**, 223–234.

Matsuura K, Nagai T, Nishigaki N, Oyama T, Nishi J, Wada H, Sano M, Toko H, Akazawa H, Sato T, Nakaya H, Kasanuki H & Komuro I (2004). Adult cardiac Sca-1-positive cells differentiate into beating cardiomyocytes. *J Biol Chem* **279**, 11384–11391.

Miki T, Nagashima K, Tashiro F, Kotake K, Yoshitomi H, Tamamoto A, Gonoi T, Iwanaga T, Miyazaki J & Seino S (1998). Defective insulin secretion and enhanced insulin action in K_{ATP} channel-deficient mice. *Proc Natl Acad Sci U S A* **95**, 10402–10406.

Miki T, Suzuki M, Shibasaki T, Uemura H, Sato T, Yamaguchi K, Koseki H, Iwanaga T, Nakaya H & Seino S (2002). Mouse model of Prinzmetal angina by disruption of the inward rectifier Kir6.1. *Nat Med* **8**, 466–472.

Nishi K, Yoshikawa Y, Sugahara K & Morioka T (1980). Changes in electrical activity and ultrastructure of sinoatrial nodal cells of the rabbit's heart exposed to hypoxic solution. *Circ Res* **46**, 201–213.

Noma A (1983). ATP-regulated K^+ channels in cardiac muscle. *Nature* **305**, 147–148.

Qu Y, Baroudi G, Yue Y, El-Sherif N & Boutjdir M (2005). Localization and modulation of α_{1D} (Cav1.3) L-type Ca channel by protein kinase A. *Am J Physiol Heart Circ Physiol* **288**, H2123–H2130.

Rosati B, Rocchetti M, Zaza A & Wanke E (1998). Sulfonylureas blockade of neural and cardiac HERG channels. *FEBS Lett* **440**, 125–130.

Saegusa N, Sato T, Saito T, Tamagawa M, Komuro I & Nakaya H (2005). Kir6.2-deficient mice are susceptible to stimulated ANP secretion: K_{ATP} channel acts as a negative feedback mechanism? *Cardiovasc Res* **67**, 60–68.

Saito T, Sato T, Miki T, Seino S & Nakaya H (2005). Role of ATP-sensitive K^+ channels in electrophysiological alterations during myocardial ischemia: a study using Kir6.2-null mice. *Am J Physiol Heart Circ Physiol* **288**, H352–H357.

Sakamoto N, Uemura H, Hara Y, Saito T, Masuda Y & Nakaya H (1998). Bradykinin B_2-receptor-mediated modulation of membrane currents in guinea-pig cardiomyocytes. *Br J Pharmacol* **125**, 283–292.

Sato T, O'Rourke B & Marban E (1998). Modulation of mitochondrial ATP-dependent K^+ channels by protein kinase C. *Circ Res* **83**, 110–114.

Seino S (1999). ATP-sensitive potassium channels: a model of heteromultimeric potassium channel/receptor assemblies. *Annu Rev Physiol* **61**, 337–362.

Seino S & Miki T (2003). Physiological and pathophysiological roles of ATP-sensitive K^+ channels. *Prog Biophys Mol Biol* **81**, 133–176.

Suzuki M, Li RA, Miki T, Uemura H, Sakamoto N, Ohmoto-Sekine Y, Tamagawa M, Ogura T, Seino S, Marbán E & Nakaya H (2001). Functional roles of cardiac and vascular ATP-sensitive potassium channels clarified by Kir6.2-knockout mice. *Circ Res* **88**, 570–577.

Suzuki M, Sasaki N, Miki T, Sakamoto N, Ohmoto-Sekine Y, Tamagawa M, Seino S, Marban E & Nakaya H (2002). Role of sarcolemmal K_{ATP} channels in cardioprotection against ischemia/reperfusion injury in mice. *J Clin Invest* **109**, 509–516.

Verheijck EE, Wessels A, van Ginneken AC, Bourier J, Markman MW, Vermeulen JL, de Bakker JM, Lamers WH, Opthof T & Bouman LN (1998). Distribution of atrial and nodal cells within the rabbit sinoatrial node: models of sinoatrial transition. *Circulation* **97**, 1623–1631.

Yao A, Su Z, Nonaka A, Zubair I, Spitzer KW, Bridge JH, Muelheims G, Ross J Jr & Barry WH (1998). Abnormal myocyte Ca^{2+} homeostasis in rabbits with pacing-induced heart failure. *Am J Physiol Heart Circ Physiol* **274**, H1441–H1448.

Acknowledgements

We are grateful to M. Tamagawa, Y. Reien and I. Sakashita for excellent technical and secretarial assistance. We thank Drs T. Ogura, H. Uemura and T. Kuwaki for valuable suggestions. This study was supported in part by Grants-in-Aid from the Ministry of Education, Science, Sports and Culture of Japan and the K. Watanabe Research Fund.